HYCELTEC 2022
VIII Symposium on Hydrogen, Fuel Cells and Advanced Batteries
Buenos Aires, July 11-14, 2022

8th Symposium on Hydrogen, Fuel Cells and Advanced Batteries, Buenos Aires, July 11th-14th, 2022

A High-performance proton exchange membrane water electrolyzer using novel fluorine-doped tin oxide-based anodes (O-6H)

S. Delgado[1,2,3*], T. Lagarteira[1,3], A. Gago[2], K. A. Friedrich[2], A. Mendes[1,3**]

[1] *LEPABE - Laboratory for Process Engineering, Environment, Biotechnology and Energy, Faculty of Engineering, University of Porto, Rua Dr. Roberto Frias, 4200-465 Porto, Portugal*

[2] *Institute of Engineering Thermodynamics/Electrochemical Energy Technology, German Aerospace Center (DLR), Pfaffenwaldring 38-40, 70569,Stuttgart, Germany*

[3] *ALiCE - Associate Laboratory in Chemical Engineering, Faculty of Engineering, University of Porto, Rua Dr. Roberto Frias, 4200-465 Porto, Portugal*

(*) Pres. author: sdelgado @fe.up.pt

(**) Corresp. author: mendes@fe.up.pt

Keywords: Electrolysis, PEMWE, Hydrogen, Electrocatalysts, Stability

1. Introduction

The deployment of technologies coupled with renewable energy sources for the sustainable production of hydrogen is a promising route to allow rapid decarbonization of the energy. Proton exchange membrane water electrolyzers (PEMWE) emerge readily for converting renewable electricity into storable hydrogen. Aside from many advantages, there are some demerits needed to be circumvented for PEMWE technology to keep up with the ambitious targets envisioned for the near future. The catalysts used for both oxygen evolution reaction (OER) and hydrogen evolution reaction (HER), typically based of Ir and Pt respectively, contribute for ca. 8-10 % of the overall balance of stack cost. Assuming a typical Ir loading of 2 $mg_{Ir}\cdot cm^{-2}$ and operation at 4 $W\cdot cm^{-2}$, nearly 500 kg of Ir is required per GW, which in turn poses a major and prohibitive roadblock for the commercialization of PEMWEs, since Ir is a scarce and expensive metal with a mere yearly production rate of < 9 ton. According to the European FCH-JU and US department of energy (DOE), the investment costs must be at least halved for PEMWE to be competitive at the GW scale applications; currently, 1000-2000 $€\cdot kW^{-1}$ shall be lowered down to 300-600 $€\cdot kW^{-1}$.

There had been several ventures to meet capital cost targets, especially concerning the development of cutting-edge, high structured novel catalysts in order to reach the energy density goal of *ca.* 0.01 $g_{Ir}\cdot kW^{-1}$ at 1.79 V, corresponding to an Ir loading reduction by a factor of 40 (0.05 $mg_{Ir}\cdot cm^{-2}$)[2]. Besides the efforts, electrochemical and morphological characterizations had enabled to decouple several triggering degradation mechanisms associated with Ir-based catalysts' instability; unanimous conjectures point out that support materials must have high surface area coupled to favour electronic/lattice interactions with Ir catalyst and enable the enhancement of both stability and OER specific activity. Lately, metal-doped SnO_2 had been assigned as good supports for IrO_2 and Ru catalysts. Doping metals such as In-, Ta-, Nb-, In- SnO_2 provide fair conductivity and a great catalyst-support interaction which offers enhanced stability to IrO_2. A recent work has delved into the possible corrosion mechanisms associated with tin-based electrocatalyst supports. The time-dependent dissolution of In, F and Sb from SnO_2:F (FTO), SnO_2:Sb (ATO) and SnO_2:In (ITO) catalysts was studied in a harsh acidic and oxidative electrolyte environment, ranging from cathodic potentials to high anodic potentials - oxygen evolution regions (-0.6 to 3.2 V_{RHE}). The FTO film was highlighted as a very promising support for catalysts due to its unmatchable stability at such conditions, surpassing both ATO and ITO [3].

The former evidence served as motivation for the present work. FTO nanoparticles were produced for the first time for serving as support to Ir nanoparticles, using a modified polyol reduction method. The microstructural properties of the support particles were analysed upon applying several heat treatments and the effect of electronic and lattice strain on the overall performance and stability of the catalyst in OER conditions was both screened in an RDE setup and in PEMWE single-cell operation. Herein, the optimum preparation routes of IrOx/FTO anodes are reported, which besides allowing to drop the loading of Ir by nearly 70 %, also ensure 1.75-fold higher performances @ 2 V and 80 °C comparatively to a cell using the state-of-the-art catalyst (IrO_2).

2. Experimental

2.1 Synthesis of the electrocatalysts and preparation of electrodes

Fluorine doped tin oxide (FTO) nanoparticles were prepared using a modified sol-gel procedure. Ethanol was added to a salt precursor of tin oxide and stirred for 2 hours. Simultaneously, distilled water and NH_4F were added dropwise into the beaker containing the previous solution. The pH of the solution was carefully controlled to alkaline pH. A white opaque precipitate was formed which consisted of the FTO nanoparticles. The solution was filtrated and dried for 4h at 60 °C. Three annealing treatments were performed placing 150 mg of as-prepared FTO powder in a tubular furnace for 4 hours under airflow (200 $mL\cdot min^{-1}$) at 300 °C, 500 °C and 700 °C. A modified polyol reduction was used to support IrO_2 salt precursor - $IrCl_3\cdot xH_2O$ (Alfa Aesar) on the prepared FTO powders, in an ethane-1-2-diol solution (pH=13), maintaining a ratio of 1:1 wt. % /wt. % between the precursor and the support, at 175 °C on a hot plate for three hours. The final catalysts were described as XIrO2/FTO_Y, where X refers to a mass fraction and Y to the annealing temperature. A catalyst ink was prepared by mixing the synthesized powders, IrO_2/FTO or commercial Pt/C which was then sprayed on top of Nafion 115 at both sides to produce catalyst coated membranes with 1 $mg_{catalyst}\cdot cm^{-2}$ at the anode side with Ir based catalysts, and 0.3 $mg_{Pt}\cdot cm^{-2}$ at the cathode side. A 4 cm^2 active area PEM water electrolyser was assembled using two Ti PTLs

with Pt coating, a hydrophilic carbon paper at the cathode side (Sigracarb 2050, Fuel CellStore) and each prepared CCM placed in the middle. A torque of 0.6 Nm was applied to 4 screws which served to clamp the cell.

2.2 Electrochemical characterization

The catalyst suspension deposited on the Au tip consisted of 20 µL containing an overall mass of metallic iridium of 2.8 ±0.1 μg_{Ir} (loading of 14.3 $\mu g_{Ir} \cdot cm^{-2}$). The working electrode was dipped into the electrolyte (0.1 M $HClO_{4(aq)}$) and conditioned in Ar during 100 cycles between 0.05 V – 1.4 V (*vs.* RHE) at 100 mV s^{-1} and 0 RPM. A cyclic voltammogram (CV) was recorded from 0.05 V to 1.4 V using a scan rate of 20 $mV \cdot s^{-1}$. Afterwards, a linear sweep voltammetry (LSV) was recorded from 1.1 V to 1.9 V *vs*. RHE at 1600 RPM to ascribe the OER mass activity of each catalyst. An accelerated stress test (AST) was performed and the OER catalytic performance of the synthetized catalysts was evaluated once again. The AST consisted of cycling the potential in the typical potential range of PEMWE cell operation (1.1 V to 1.8 V) for 10 000 cycles at a scan rate of 100 $mV \cdot s^{-1}$. Each PEM electrolyser containing the prepared CCMs was characterized by performing a polarization curve at 60 °C, and by retrieving electrochemical impedance spectra in galvanostatic mode (8 A). To assess the stability of the best performing system, a chronopotentiometry was recorded at 1.3 A cm^{-2} for 320 h and 75 °C.

3. Results

3.1 Electrocatalytic OER performance of IrOx/Fluorine doped SnO_2 supports using RDE

Fig.1 displays the cyclic voltammograms recorded at 20 $mV \cdot s^{-1}$ for the all-synthesized electrocatalysts and the commercial unsupported IrO_2 from PREMETEK. The CV spectra show that depending on the type of support, the initial Ir valence states differ from one another due to the peaks arising at different potentials. All synthesised catalysts reveal that mainly hydrous Ir oxide (IrO_x - 0.6 V to 1.0 V *vs*. RHE) was generated; these catalysts are amorphous and possess more defects in comparison to crystalline materials, therefore are expected to have higher activities and enhanced usage of Ir active sites. On the other hand, there is no evidence of metallic Iridium redox pairs in none of the synthesised electrocatalysts, which typically appear at potentials below 0.4 V *vs.* RHE. Whilst the FTO based catalyst annealed at 500 °C depicts the earliest onset tendency for OER activity at more oxidative potentials, the catalyst annealed at 300 °C presents the best activity for hydrogen evolution. Moreover, the larger anodic peak current density reached for the sample $30IrO_2$/FTO_500 and the quasi-symmetric redox peaks, with no substantial peak potential separation unveil that this catalyst is mostly reversible with a larger number of active Ir trivalent/tetravalent species.

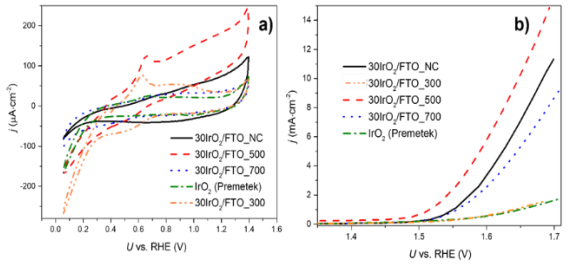

Fig. 1. OER characterization of $XIrO_2$/FTO_Y in RDE setup by means of a) CVs retrieved at 20 $mv \cdot s^{-1}$ and b) OER LSVs recorded at 2 $mV \cdot s^{-1}$ in an Ar saturated 0.1 M $HClO_4$ solution at 25 °C. The loading of Ir catalyst was kept at 14.2 $\mu g_{Ir} \cdot cm^{-2}$ in the 0.196 cm^2 Au WE tip at 1600 RPM.

Fig.1 b) displays the LSVs corresponding to the OER performance of the prepared electrocatalysts. The Ir NPs supported in FTO annealed at 500 °C unveil the earliest onset and therefore highest OER mass-activity (MA) at 1.51 V, Table 1. All the synthetized electrocatalysts outperformed the commercial catalyst in terms of catalytic activity, except for $30IrO_2$/FTO_300. The measured OER activities measured at an overpotential of 280 mV, approached the best values attained in the literature and even outperformed the most ambitious commercial catalysts, especially, $30IrO_2$/FTO_500 which delivers a 5-fold higher OER activity at 1.51 V vs. RHE comparatively to the commercial catalyst (77 $A \cdot g^{-1}$ *vs.* 15.5 $A \cdot g^{-1}$ at 25 ◦C, 1600 RPM in 0.1 M $HClO_4$). These results suggest that dispersing Ir nanoparticles in FTO is beneficial to decrease the activation energy barrier of OER and there is an optimum degree of calcination/annealing temperature for boosting the beneficial support features, which happens at 500 ◦C, Table 1.

Table 1. Data regarding OER mass activity of prepared catalysts and specific MA variation upon AST of 10 k cycles.

Catalyst	OER activity @ 1.51 V ($mA \cdot cm^{-2}$)	Tafel Slope ($mV \cdot dec^{-1}$)	OER activity variation upon the AST (+/- %)
IrO_2	15.5	83.7 ± 4	- 50
$30IrO_2$/FTO_NC	27	63.8 ± 7	- 41
$30IrO_2$/FTO_300	6.9	186 ± 4	+ 74.3
$30IrO_2$/FTO_500	77	59 ± 1	+ 0.41
$30IrO_2$/FTO_700	17	64.8 ± 6	- 25.5

Tafel slope values were obtained at a steady-state current density, in the overpotential window of 0.25 V < η <0.45 V. The smallest slope value was achieved for the catalyst $30IrO_2$/FTO_500 with solely 59 $mV \cdot dec^{-1}$, followed by 63.8 $mV \cdot dec^{-1}$ ($30IrO_2$/FTO_NC), 64.8 $mV \cdot dec^{-1}$ ($30IrO_2$/FTO_700), 83.4 $mV \cdot dec^{-1}$(IrO_2) and finally 186 $mV \cdot dec^{-1}$ ($30IrO_2$/FTO_300). The Tafel slope of the commercial catalyst falls in the typical range of such types of catalysts reported in the literature [5,6]; the lower Tafel slopes also indicate that the reaction faces a chemically controlled kinetics unlikely to $30IrO_2$/FTO_300 which presents a higher Tafel slope indicating that the limiting step faces a competition between a chemically governed and

an electron transfer mechanism. The latter suggests the support annealing step at 300 ◦C might have condemned the initial microstructure providing insulating properties instead of electrically conductive features. The accelerated stress test produced distinct OER end of life activities depending on the type of annealed FTO support. In fact, the cycling increased the activity of the former worst-performing catalyst, 30IrO_2/FTO_300 in *ca.* 74 %; yet, no significant OER activity variation was noticed for the catalyst 30IrO_2/FTO_500, which suggests that this catalyst is highly stable under harsh acidic OER conditions. Regarding the non-calcined and calcined support at the highest temperatures, 700°C, the OER MA loss was 41 % and 25.5 %, respectively, suggesting that the catalyst-support interaction was detrimental and the corrosion of the support was triggered influencing the activity of the Ir NPs, see Table 1.

3.2 PEMWE performance

Comparatively to the benchmark IrO_2 catalyst, all prepared anodes with an overall loading of 0.3 mg_{Ir}/cm^2 based of FTO demonstrate much lower overpotentials, especially at the activation (< 200 mA·cm^{-2}) and ohmic overpotential regions, Fig 1a). The use of FTO nanoparticles allows the improvement of the in- and through-plane electrical conductivity of the catalyst layer, thus allowing to circumvent the major problems verified with other less stable and less conductive ATO or ITO based anode layers. The EIS spectra recorded at 2 A·cm^{-2}, Fig.2b) show that there is an evident decrease on the charge transfer resistances associated with the OER reaction for the Ir catalysts dispersed in FTO nanoparticles (500 °C, 700 °C). Minor mass-transport resistances are noticed for Ir dispersed in FTO nanoparticles annealed at 500 °C compared to the Ir commercial catalyst.

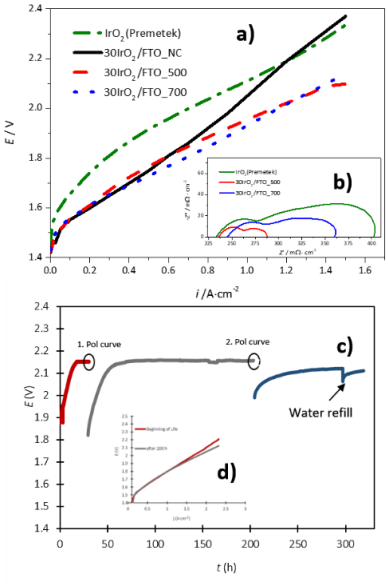

Fig. 2. PEMWE performance and stability using IrO_2 and 30IrOx/FTO_Y (NC/500°/700°) CCM anodes in a cell with N117 at 60 °C); b) EIS recorded at 2 A·cm^2; c) long-term chronopotentiometry at steady 1000mA·cm^{-2} d) Pol curves recorded at BoL and after 200 h of operation @ 75 °C.

The cell was subjected to a chronopotentiometry at high current densities - 1.3 A·cm^{-2}, for over 320 h and the overpotential of the cell was kept constant at η=0.82 V, thereafter no visible triggered degradation mechanisms, such as the dissolution of fluorine ions, are attributed to anodes composed of FTO nanoparticles prepared under an annealing step at 500° C, as evidenced in Fig. 2c. After 200 h of continuous operation, the current density of the cell even improved substantially suggesting the enhancement of water-gas management was probably due to further rearrangement of the catalyst layer microstructure, Fig. 2d.

4. Conclusions

Iridium oxide nanoparticles were successfully nucleated in synthetized FTO nanoparticles with an optimum size of the metal particles of *ca*. 4.75 nm. FTO nanoparticles prepared under an annealing step of 500 °C in airflow, boosted electrical and microstructural features; besides lowering the loading of Iridium in 70 % in the anode of a PEMWE, the performance of the cell was improved in *ca.* 75 % at 2 V, 60 °C when using anodes of FTO annealed at 500 °C, compared with IrO_2 anodes. The calcination temperature was found to deeply influence the morphology and activity of iridium electrocatalysts supported on FTO. All electrochemical evidences were supported by physicochemical characterization (HR-TEM, XPS, TGA, EDS). The results accomplished, provide critical perspectives for the future preparation of high-performing cost-effective and sustainable PEMWEs, thus enabling the clean and efficient energy production and storage opportunities.

Acknowledgements

This work was financially supported by LA/P/0045/2020 (ALiCE), UIDB/00511/2020 and UIDP/00511/2020 (LEPABE), funded by national funds through FCT/MCTES (PIDDAC). The authors acknowledge the financial support of the project Baterias 2030, with the reference POCI-01-0247-FEDER-046109, co-funded by the Operational Programme for Competitiveness and Internationalisation (COMPETE 2020), under the Portugal 2020 Partnership Agreement, through the European Regional Development Fund (ERDF). Sofia Delgado acknowledges FCT for the doctoral grant with reference SFRH/BD/144338/2019.

References

[1] A. Marshall, B. Børresen, G. Hagen, M. Tsypkin, R. Tunold, Energy 32 (2007) 431–436.

[2] S. Siracusano, V. Baglio, A. Stassi, R. Ornelas, V. Antonucci, A.S. Aric, Int. J. Hydrogen Energy 36 (2011) 7822–7831.

[3] S. Geiger, O. Kasian, A.M. Mingers, K.J.J. Mayrhofer, S. Cherevko, Sci. Rep. 7 (2017) 1–7.

[4] J. Gaudet, A.C. Tavares, S. Trasatti, D. Guay, Chem. Mater. 17 (2005) 1570–1579.

[5] Y. Zhu, W. Zhou, Y. Zhong, Y. Bu, X. Chen, Q. Zhong, M. Liu, Z. Shao, Adv. Energy Mater. 7 (2017) 1602122.

[6] M. Blasco-Ahicart, J. Soriano-Lopez, J.J. Carbo, J.M. Poblet, J.R. Galan-Mascaros, Nat. Chem. 2017 101 10 (2017) 24–30.